

# Chapter 2

## Fusion of Photos Captured with Exposure Bracketing

### 2.1 Introduction

#### 2.1.1 What Is High Dynamic Range Imaging?

Usually the terms “High Dynamic Range” (HDR) and “High Dynamic Range Imaging” (HDRI) are used whenever the lightness intensity values span four or more orders of magnitude. A related term, “low dynamic range (LDR)”, refers to digital systems supporting only eight bits per colour channel or intensity ratios between 0 and 255.

HDRI is an emerging field. It is guided by recent electronic industry trends that lead to further miniaturization of compact Digital Still Cameras (DSCs) and increase the image pixel resolution, making the sensor smaller and causing it to suffer from a lower dynamic range due to its reduced capacity. On the other hand, consumer demand for increased image quality and attractiveness is forcing manufacturers to develop more sophisticated image-processing algorithms.

The visual quality of high dynamic range images is much higher than that of conventional low-dynamic-range images. With the development of this technology, it will become the norm rather than the exception.

The main challenges of HDR technology are capturing, storing, and displaying/printing images. When taking photographs of an outdoor scene, the brightness ratio, or dynamic range, between an area in full sunlight and another area in deep shade can exceed 10,000:1. Cameras with charge-coupled device (CCD) imaging sensor are able to deal with dynamic ranges of up to 2500:1, and when a reflective print of this scene is created, the print is typically limited to a dynamic range of about 100:1. The human eye can accommodate luminance in a single view over a range of about 10,000:1, is capable of distinguishing about 10,000 colours at a given brightness, deals with such high dynamic range scenes by adapting locally to each part of the scene, and thus is able to retrieve details from low-luminance as well as high-luminance areas.

In still photography, HDR can be used to create images from scenes that have a broad range of tonal values from shadows to highlights. This situation is typical of landscapes and scenes with illuminants, since such scenes may have a dynamic range of 100,000:1 or more. Besides traditional landscapes, other outdoor images that might benefit from HDR include those with significant highlights such as strongly lit reflective surfaces. HDR can also be applied to good effect with indoor or outdoor architectural photography, where natural and artificial light combined with shadows can produce a wide dynamic range over various materials and surfaces.

However, there is no guarantee that the HDR technique by itself can produce a “better” interpretation of a given scene. For decades, photographers made decisions on what is really important, by composing and exposing, and leaving the rest behind.

As can be seen, HDR is not only the bit size of images to be stored. In the process of acquiring digital images, sensors have to possess higher capacities so that more gradations of light can be represented and true gradations of scene lightness are not spoiled by noise spikes.

Now, the problem consists of compressing the dynamic range so that highlights are not overexposed and shadows are not too dark. This problem becomes more essential in photo printing technology. Because of the large mismatch between the dynamic range of the print paper and the original scene, there needs to be some mapping or transformation of the dynamic range of the scene onto the available dynamic range of the print paper to create a pleasing reproduction. Simple scaling will not produce the desired result, because a large volume of lightness gradations will be lost.

### ***2.1.2 Hardware Solutions***

Fujifilm Super CCD SR. In January 2003, Fujifilm announced the new SuperCCD SR sensor type. The SuperCCD SR (Super Dynamic Range) offers almost two stops more dynamic range than conventional CCD. Beneath each microlens on the sensor surface (a photosite) are two photodiodes: the primary one captures dark and normal light levels (more sensitive) and the secondary one captures brighter details (less sensitive). The signals from the two photodiodes are intelligently combined by the camera to deliver an image with an extended dynamic range. This combination of primary and secondary photodiodes produces an image that is more richly detailed than conventional CCDs, resolving more detail in the highlight and dark areas of the image.

BrightSide Technology HDR Display. BrightSide Technology introduced the DR37-P that uses an array of individually modulated LED backlights to provide 10 times the brightness and 100 times the contrast of existing televisions and computer monitors. BrightSide’s Extreme Dynamic Range display delivers more vibrant images and makes it possible to see the data in vivid detail. In 2007, BrightSide

Tech was acquired by Dolby Laboratories. Currently, the modern technology Dolby Vision allows the creation of 12-bit depth content that is ready to be viewed on compatible displays and TVs.

Modern trends in the TV industry include the creation of the HDR10 standard supporting 10-bit depth contents. In 2017, in Consumer Electronics Show (CES) all the major TV manufactures demonstrated TVs that allow 10-bit video content to be viewed; some of them, such as LG and Sony, are able to deal with Dolby Vision content.

The Canon PROGRAF iPF5000 colour inkjet printer appeared on the market in May 2006. It was the first high-end inkjet printer to offer a 16-bit printer driver and is a non-standard plug-in for Photoshop because Windows printer drivers are restricted to an eight-bit path. The plug-in processes the image in 16-bit mode and then sends it to the printer as 12-bit data. The goal of this is to expand the dynamic range of the reproduced image and surprisingly also the gamut. There is some debate about whether the Canon 16-bit mode truly offers a benefit or not. Even as display technology pushes along towards HDR, ink on paper will remain an LDR medium. To make great prints from truly “high” dynamic range images will take a lot of effort in tone mapping.

Epson Surecolor P series printers were announced in 2015 and incorporate a reformulated Epson UltraChrome HDX 10-colour ink set for commercial and flexographic printers, as well as graphic designers, photographers, and fine art reproduction houses.

### ***2.1.3 Main Challenges***

When the dynamic range is less than the contrast in an actual scene, the image sensor may become saturated. When that happens, the image sensor cannot capture details from bright and dark areas of such an image at the same time. Adjusting or increasing the sensitivity of the dark areas may result in over-saturation of the bright areas, and conversely, adjusting or increasing the sensitivity of the bright areas may result in over-saturation of the dark areas. One of the possible approaches is to use exposure bracketing to take several shots: underexposed, normal, and overexposed.

During photo shooting, the camera may occasionally be translated or rotated; therefore, prior to processing, the images must be co-aligned, or registered, taking into account optical distortions of the camera’s lenses.

In the case of linear scaling of the image to fit eight bits, a serious loss of contrast may occur. To avoid this, a sophisticated tone-mapping technique should be applied.

Another problem is adequately processing colour channels to avoid colour distortions.

The preservation of the scene’s dynamic range is a critical problem in panorama creation. Very often outdoor panoramas have very large variations of lightness, so mapping to LDR image helps to preserve details in overall scene.

## 2.2 Proposed Method of Dynamic Range Compression

In this work, we considered the problem of lost details in the images captured with low dynamic range sensors. The main idea is to use several images captured with exposure bracketing. This means that one of the images has normal exposure, and several other images are over- or underexposed. The method is aimed at photos shot by regular consumer cameras. Recent trends in the electronic industry have led to the miniaturization of compact DSCs, and thus the sensors have become smaller and suffer from a low dynamic range due to their reduced capacity. A side effect of this process is the amplification of noise, especially in shadow areas, so that details of the image in shadows are completely lost. Oversaturation of image sensors leads to flat white patches. One way to avoid a loss of details in shadow and highlight areas is to capture several images with exposure bracketing to preserve highlight details in underexposed images and shadow details in overexposed images. Note here that colour representation also suffers in shadowed and highlighted areas. The final image should contain as much detail as possible from the entire set of bracketed images.

Usually, exposure bracketing mode is present in modern consumer cameras, so it is possible to shoot a set of differently exposed images in a relatively small period of time. However, usually the camera will shake or move during capture, leading to some translations between captured images. Additionally, some distortion may be present due to the imperfect optical system of a DSC. Hence the first necessary step is to align all images of the set, taking into account optical distortion.

The main problem in preserving details of the image is matching the dynamic range of the scene being captured to the display or printing device. The application of simple linear stretching will inevitably lead to a loss of local contrast, and the final image will look flat. The main challenge is therefore to compress the dynamic range while preserving local contrast, that is, to apply a special tone mapping technique. A very common problem of various local mapping operators is the formation of a halo around very steep edges in cases when the subject to be captured has some light emitting sources behind. This problem is addressed by Safonov et al. (2006).

In summary, the following problems exist.

- Translations between images, which also lead to different distortions due to the optical system.
- Insufficient data for camera profile reconstruction and HDR image formation.
- Loss of details in low dynamic range images.
- Loss of contrast as a result of dynamic range compression.
- Halo formation around very steep edges.
- Preservation of colours from all images of the set.

### 2.2.1 Registration

The first step in image formation is registration of all images in the set with one chosen reference image. Possible image transformations in the case of hand shooting are translation and rotation as well as correction of optical distortion.

A detailed description of the registration method is outside the scope of this work.

### 2.2.2 Fusion

The next step is fusion of the registered images. Images with different exposures can be fused together using a sophisticated method of camera calibration and recovery of the true HDR image. One of the first papers dedicated to the reconstruction of a nonlinear camera response profile was published by Mann and Picard (1995) and Mann and Mann (2001). The authors addressed the problem of a nonlinear response curve but provided a rather limited method of recovering it. They used several fully aligned images captured with exposure bracketing and reconstructed the curve using polynomial representation (Fig. 2.1).

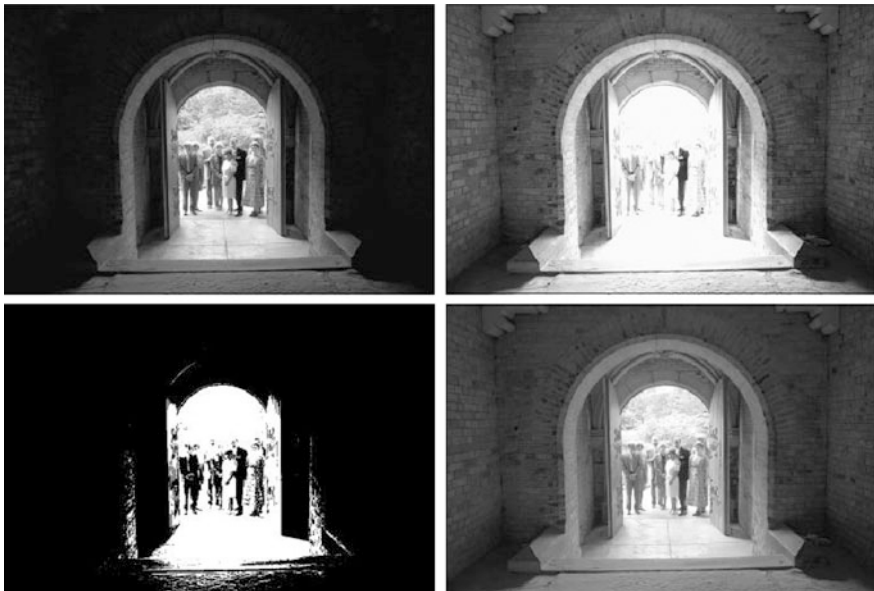


**Fig. 2.1** Mann and Picard (1995) used several fully aligned images captured with exposure bracketing and reconstructed the curve using polynomial representation

In the two reference methods described above, an HDR image itself is not formed but a calibration step is necessary. Work on recovering the camera response profile was continued by Debevec and Malik (1998). Their method has become widespread among researchers as well as among users who work with HDR still images, having sets with images captured with exposure bracketing. Instead of some abstract units for lightness, here the authors propose a physically based model for recovering the camera response profile. It is assumed that known pixel values  $Z$  are the result of exposure of the sensor to the irradiance  $E$  during some known exposure time  $t$  using the mapping function  $f$ .

$$Z_{ij} = f(E_i \Delta t_j),$$

$$g(Z_{ij}) = \ln E_i + \ln \Delta t_j, \quad \text{where} \quad g \equiv f^{-1},$$

and the problem of response curve reconstruction is reduced to the least squares problem of recovering unknown  $g$  and  $E_i$ .

To recover the camera response profile, it is necessary to have multiples of images with known priors, such as the exposure time, in order to have enough data for smooth curve recovery. If the number of images is insufficient to calibrate the camera, the problem of high dynamic compression consists of preserving details that are present in all images.

Very interesting works have been done on the problems of combining differently exposed images or even combining images of a different nature. Perez et al. (2003) extended an idea proposed by Fattal et al. (2002) concerning the recovery of an image using its gradient. Basically, the problem consists of approximating an image using its gradient, that is, by minimizing the misfit between a known gradient  $G$  and the gradient of the target image  $I$  in the least squares sense:

$$\iint \|\nabla I - G\|^2 dx dy \rightarrow \min.$$

Here  $I$  is an unknown image and  $G$  is its known gradient. If the norm of the difference is represented as

$$\|\nabla I - G\|^2 = \left( \frac{\partial I}{\partial x} - G_x \right)^2 + \left( \frac{\partial I}{\partial y} - G_y \right)^2,$$

this equation leads to the well-known Poisson equation:

$$\Delta I = \text{div} G.$$

Usually, a Laplace operator is approximated with a finite difference operator, and this in turn leads to a system of linear equations, which can be solved using various methods.

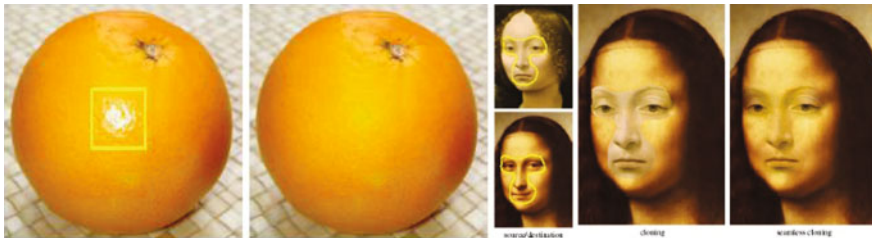


**Fig. 2.2** Seamless cloning by Fattal et al. (2002)

**Fig. 2.3** Night-time and daytime images are fused together using gradients (Raskar et al. 2004)



Based on this method, Fattal et al. (2002) developed various techniques of image processing such as seamless cloning and image editing (see Fig. 2.2). Note here that more operations are possible using gradients such as rotation, affine transforms, noise suppression, combining images with different depths of field, and so on.

The idea of employing image gradients was elaborated by Raskar et al. (2004) and Ilie et al. (2005). The authors describe a method of enhancing images, obtained from, for example, surveillance video cameras, where objects are captured under different lighting conditions (daylight and night-time images); see Figs. 2.3 and 2.4.

They first construct the image using the weighted sum of gradients of input images based on the “pixel importance” computed from the local variance. After that, they apply the technique described by Fattal et al. (2002) in the gradient domain or methods from Durand and Dorsey (2002) and Reinhard et al. (2002) in the image domain to compress the dynamic range of the resulting image.

In the paper by Socolinsky (2000), the problem of recovering an image using a known gradient is addressed in more detail. The author points out the very important problem of local contrast reduction that occurs as a result of dynamic range compression. The author proposes to perform optimization under constraints for luminance values.



**Fig. 2.4** Night-time and daytime images are fused together using gradients (Raskar et al. 2004)

The method presented by Fattal et al. (2002) was originally applied to the HDR image. The authors first computed gradients of the input HDR image, then performed the reduction of gradients by multiplying them by the gradient attenuation function, and finally reconstructed the image using processed gradients.

In a set of differently exposed photos, some images may look dark but have details of highlighted areas of the captured scene, while some images may look too bright but have details in shadowed areas of the scene. Since the human visual system is mostly aimed at details, that is, local changes of lightness, as mentioned by DiCarlo and Wandell (2000), the gradient of the input images must be properly preserved. The main idea is to take highlight details from dark images and shadow details from bright images. For this purpose, an image gradient consisting of maximal magnitudes of gradients of input images is created, and after that (following some tone mapping), lightness values are reconstructed using the Poisson equation (Tolstaya et al., 2009).

Suppose we have a set of images  $\{I\}_{k=1}^K$  of the same size,  $M$  by  $N$  pixels. Let  $\{Y\}_{k=1}^K$  be the corresponding lightness channels of the input images. A fused gradient  $G^{HDR}(i, j)$  is constructed using the gradients of each individual image  $G^k(i, j)$  in the following way:

$$\begin{cases} G_x^{HDR}(i, j) = \left\{ G_x^p(i, j) \middle| |G_x^p(i, j)| = \max_{k=1..K} |G_x^k(i, j)| \right\} \\ G_y^{HDR}(i, j) = \left\{ G_y^p(i, j) \middle| |G_y^p(i, j)| = \max_{k=1..K} |G_y^k(i, j)| \right\} \end{cases},$$

where

$$G^k(i, j) = \{G_x^k, G_y^k\}_{ij}.$$

If there is no shift or rotation between images, gradients are computed using the following formulas:



$$\begin{cases} G_x^k(i,j) = Y^k(i+1,j) - Y^k(i,j) \\ G_y^k(i,j) = Y^k(i,j+1) - Y^k(i,j) \end{cases}.$$

If images are not registered, it is necessary to register them.

### 2.2.3 Mapping

Tone reproduction (also known as tone mapping) provides a method of scaling (or mapping) luminance values in the real world to a displayable range. Tone reproduction is necessary to ensure that a wide range of light in a real-world scene is conveyed on a display with limited capabilities.

Tone mapping was developed for use in television and photography, but its origins lie in the field of art, where artists make use of a limited palette to depict high contrast scenes.

Usually, the image is calibrated in advance to determine the illumination in physically based units in order to assure accurate reproduction of tone. This is especially true when speaking about night-time shots, which can be mapped as daylight scenes, if uncalibrated. However, it is possible to use heuristics to infer lighting conditions for scenes depicted by uncalibrated images. In particular, a histogram can reveal whether an image is dark overall irrespective of the actual values in the image.

The problem of tone reproduction is still a matter of intensive research interest. Many solutions have been proposed but still none of them can be universally applied. The problem of tone reproduction remains a vital one, especially in the printing area, because paper is not capable of emitting light and this will never become possible.

The majority of tone reproduction operators can be classified into the following two types: global, also known as single-scale or spatially uniform; and local, also known as multi-scale or spatially varying (see Ferwerda 1998; DiCarlo and Wandell 2000; Devlin 2002). Global operators apply the same transformation to every pixel. A global operator may depend upon the contents of the image as a whole, as long as the same transformation is applied to every pixel. Conversely, local operators apply a different scale to different parts of an image.

As noted by Fattal et al. (2002), high intensity drops lead to large gradients, so to compress the dynamic range, it is necessary to attenuate its magnitude. Here the authors propose to use different image scales to identify large gradients. They construct a Gaussian pyramid of an input HDR image and identify a large gradient at each scale. As a result, they construct a gradient attenuation function.

We propose to use bilateral filtering of an image  $Y^s$  constructed as the sum of lightnesses of all input images divided by their number:

$$Y^s = \frac{1}{K} \sum_{k=1}^K Y^k.$$

A bilateral filter proposed by Tomasi and Manduchi (1998) will smooth small variations of lightness and preserve strong edges.

$$Y^f = \frac{\sum_{k,l} Y_{i+k,j+l}^s w\left(\left|Y_{i+k,j+l}^s - Y_{i,j}^s\right|\right) h(i,j)}{\sum_{k,l} w\left(\left|Y_{i+k,j+l}^s - Y_{i,j}^s\right|\right) h(i,j)},$$

where  $w(x) = \left(1 - \left|\frac{x}{\sigma_R}\right|^2\right)^2$  is the kernel for range processing,  $h(i,j) = \exp\left(-\frac{i^2 + j^2}{2\sigma_D^2}\right)$  is a window function, and  $\sigma_D$  and  $\sigma_R$  are the standard deviations for the domain and range, respectively. Here it is proposed to set  $\sigma_D$  as large as 100 to achieve smoothing of small variations of lightness. As for  $\sigma_R$ , here it is controlled by the size of the input images and varies between 10 and 50.

After that, a gradient  $\mathbf{G}^f = \{G_x^f, G_y^f\}$  of the filtered image is computed. This gradient will have a large magnitude at strong edges and a small magnitude in smooth or textured areas. The magnitude of the gradients of the filtered image is processed so that it spans an interval between 0.1 and 1. The gradient attenuation function is formed using computed values, as follows:

$$\Phi = \left(1 - \left(\frac{1}{1 + |G_x^f| + |G_y^f|}\right)^{0.5}\right)^\gamma,$$

where gamma is usually set to 1, but in some extreme cases can reach values greater than 1 and smaller than 3. The greater gamma is, the more intense the gradient attenuation that occurs: strong edges will be attenuated more than weak edges. Constant multipliers of the new gradient field will not affect the results. This means that the scale of the gradient attenuation function does not matter.

The new gradient field (“low dynamic”) is the product of this function and the initial fused gradient:

$$\mathbf{G}^{LD}(i,j) = \Phi(i,j) \mathbf{G}^{HDR}(i,j).$$

This transformation allows attenuation of strong edges, thus compressing the dynamic range of an image.

To recover the image intensities, a Poisson equation has to be solved. Here an image is approximated using its gradient; that is, the misfit between the known gradient  $\mathbf{G}$  and the gradient of a target image  $\nabla I$  is minimized in a least squares sense, which leads to the Poisson equation (as mentioned above):

$$\Delta Y = \text{div} \mathbf{G}^{LD}.$$

The Laplace operator is approximated with a finite difference operator, and this in turn leads to a system of linear equations that can be solved using various methods.

The Laplace operator is approximated as follows:

$$\Delta Y(i, j) \approx Y(i+1, j) + Y(i-1, j) + Y(i, j+1) + Y(i, j-1) - 4Y(i, j).$$

The gradient (as explained above) is computed using the forward difference:

$$\nabla Y(i, j) \approx \{Y(i+1, j) - Y(i, j); Y(i, j+1) - Y(i, j)\},$$

and for  $\text{div}$ , the backward difference is applied:

$$\text{div} \mathbf{G} \approx G_x(i, j) - G_x(i-1, j) + G_x(i, j) - G_x(i, j-1).$$

Note here that the integration of gradients involves scale and translation ambiguity. That is why the resulting image  $I$  is first scaled between minimum and maximum over all images in the set. After that, every pixel of the resulting image is forced between the corresponding pixels in the entire set:

$$Y^{scaled}(i, j) = \begin{cases} M(i, j), & \text{if } Y(i, j) > M(i, j) \\ m(i, j), & \text{if } Y(i, j) < m(i, j) \\ Y(i, j), & \text{otherwise} \end{cases}$$

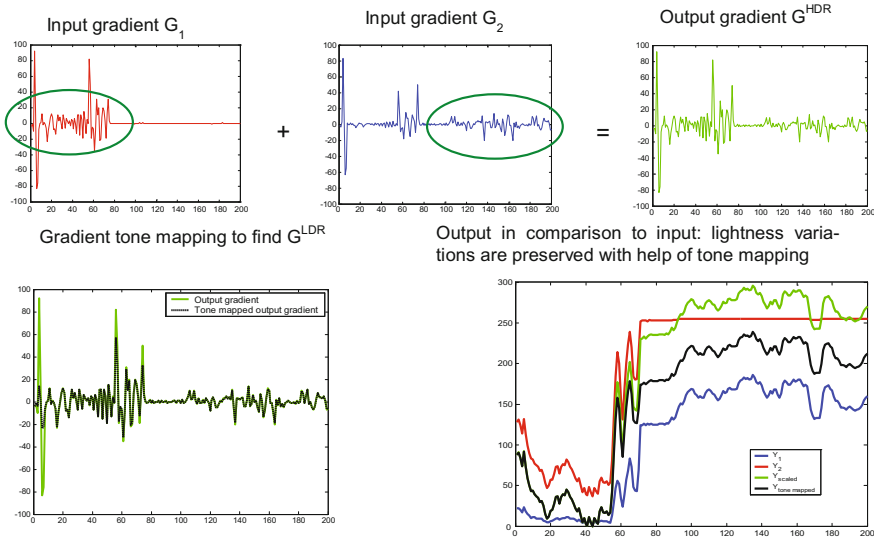
where  $M(i, j) = \max_{k=1 \dots K} \{Y^k(i, j)\}$  and  $m(i, j) = \min_{k=1 \dots K} \{Y^k(i, j)\}$ .

Figure 2.5 illustrates the process in a one-dimensional (1D) case: first, gradients having maximal magnitudes are combined to get  $\mathbf{G}^{HDR}$ . After that,  $\mathbf{G}^{HDR}$  is tone mapped to find  $\mathbf{G}^{LDR}$ . When it has been recovered and scaled, the new gradient preserves lightness variations.

### 2.2.4 Colour Processing

Most tone reproduction operators attempt to reduce an image in dynamic range, while keeping the response of human visual system to the reduced set of intensities constant. This leads to various approaches that aim at preserving brightness, contrast, and so on.

However, it is a common practice for tone reproduction operators to exclude comprehensive treatment of colours. Most operators derive a luminance based channel from input RGB values and then compress the luminance channel. However, this may change in the near future, since the fields of colour-based



**Fig. 2.5** The process in the 1D case: first, gradients having maximal magnitudes are combined to get  $G^{\text{HDR}}$ . After that  $G^{\text{HDR}}$  is tone mapped to find  $G^{\text{LDR}}$

modelling and tone reproduction are growing closer together. This can be seen in the multiscale observer model by Pattanaik et al. (1998) and in the more recent iCAM (image Colour Appearance Model) in Fairchild and Johnson (2002, 2003), and Akyuz and Reinhard (2006).

Usually, colour processing can be attributed to two main types:

(I) Colour processing of such a type is usually applied in methods involving camera calibration and construction of an HDR image with an enlarged bit rate.

Colour processing is performed in the following way: the lightness component is compressed and colour channels are computed by preservation of the ratio between them (as in Fattal et al. 2002; Mann and Pickard 1995; Mann and Mann 2001; and others).

$$\begin{bmatrix} R_{out} \\ G_{out} \\ B_{out} \end{bmatrix} = \begin{bmatrix} \frac{R_{in}}{Y_{in}} Y_{out} \\ \frac{G_{in}}{Y_{in}} Y_{out} \\ \frac{B_{in}}{Y_{in}} Y_{out} \end{bmatrix},$$

where  $R_{in}$ ,  $G_{in}$ ,  $B_{in}$ , and  $Y_{in}$  are the input colour and lightness channels respectively, and  $R_{out}$ ,  $G_{out}$ ,  $B_{out}$ , and  $Y_{out}$  are the processed colour and lightness channels respectively. This technique makes it possible to minimize colour translations before and after compression. Fattal et al. (2002) also included some parameter  $s$  to control the saturation:

$$C_{out} = \left( \frac{C_{in}}{Y_{in}} \right)^s Y_{out},$$

where  $C$  takes values of  $R$ ,  $G$ , or  $B$ . When  $s$  decreases, the saturation decreases too.

An alternative method is to convert an image to YCrCb colour space, compress the luminance, and convert the image back to RGB, if necessary. In Chap. 1 we described a method of adjusting the chromaticity channels in YCrCb, which makes it possible to avoid colour desaturation as a result of lightness channel modification.

(II) This type of colour processing is more typical for methods of fusion of colour images. Since the actual HDR image is not computed, three colour channels are processed independently and similarly to each other, as in Perez et al. (2003), Raskar et al. (2004), and so on.

A solution proposed in US patent 6,078,357 for an “image mixing circuit” by Yamamoto et al. (Matsushita Electric Industrial Co., Ltd.) uses a similar method for mixing colour-difference channels as for luminance mixing, that is, weighted summation of overexposed and underexposed images:

$$Y_{mix} = Y'_{short} \times Y_{cont} + Y_{long} \times (1 - Y_{cont}),$$

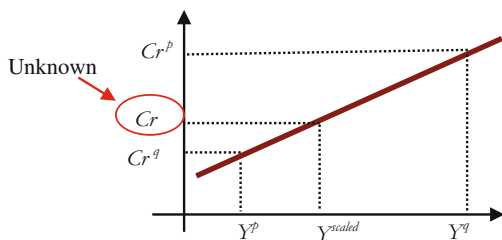
where  $Y_{mix}$  is the output luminance component,  $Y_{long}$  and  $Y_{short}$  are long and short exposure luminance components, respectively,  $Y_{cont}$  is the control signal, and  $Y'_{short}$  is the short exposure luminance component, boosted up to the level of the  $Y_{long}$  component.  $Y_{cont}$  is obtained by application of LPF to  $S_{long}$  (long exposure image signal), and then a constant and clipping are added. Note again that colour components are treated similarly.

The disadvantages of these methods are that in the first case an HDR image is required to compute ratios between colour channels or in the second case colour translations are possible due to inaccuracy of computation.

Therefore, a different method is proposed that performs linear (or quadratic or cubic) interpolation between input chromaticity channels for every pixel and then computes the new chromaticity values using the new lightness values (Fig. 2.6):

$$C_r = \frac{C_r^p - C_r^q}{Y^p - Y^q} (Y^{scaled} - Y^p) + C_r^p,$$

**Fig. 2.6** Computation of chromaticity  $C_r$  using input lightness values  $Y^p$ ,  $Y^q$ , and  $Y^{scaled}$  and known  $C_r^p$  and  $C_r^q$



$$C_b = \frac{C_b^p - C_b^q}{Y^p - Y^q} (Y^{scaled} - Y^p) + C_b^p,$$

In the case when  $Y^p = Y^q$ , chromaticity is computed as the mean between  $C^p$  and  $C^q$ . This approach makes it possible to smoothly interpolate chromaticity for the output image, since  $Y^{scaled}$  always lies between the minimum and maximum of the input images.

This method is quite effective, does not require significant computational effort, and produces pleasing results.

### 2.2.5 Results

This section presents the results of the described method as well as some discussions and future directions.

Figure 2.7 shows an example of initial panorama images captured with exposure bracketing (Vogl):

Figures 2.8 and 2.9 present the final coloured image of the panorama and the gradient attenuation function for this panorama.



**Fig. 2.7** Panorama images captured with exposure bracketing (Vogl)



**Fig. 2.8** Final coloured image of panorama obtained by the described method



**Fig. 2.9** Gradient attenuation function for the panorama image

As can be seen, strong edges will be attenuated more than weak edges. Constant multipliers of the new gradient field will not affect the results. This means that the scale of the gradient attenuation function does not matter.

Capturing waterfalls during bright days while preserving the texture and surroundings is a very challenging problem. Figure 2.10 shows the results of combining waterfall images.

Figures 2.11 and 2.12 show the results of mapping of a thermal area, including bright vapour trails and a waterfall.

Figure 2.13 is an example provided by the Photomatix website.

In general, as we can see, a method involving calibration can result in light areas in the final image that are brighter than the same areas in all input images. This drawback can be seen in the window curtain. The same is true for bright areas: if an area is bright throughout the whole of the image set, in the final image it can appear darker, which can be seen in the area where light from the window falls on the floor.

In the proposed method, the final image brightness is controlled by the input images: in the case of an underexposed set of input images, the result will look dark as well. (However, in this case histogram stretching is usually applied, although this step can be omitted.) Uneven distribution of exposures in input images will result in unnatural-looking images with over-brightened and over-darkened parts, since the method is aimed at images sets produced by consumer cameras in “exposure bracketing” mode, which is usually characterized by constant exposure steps.

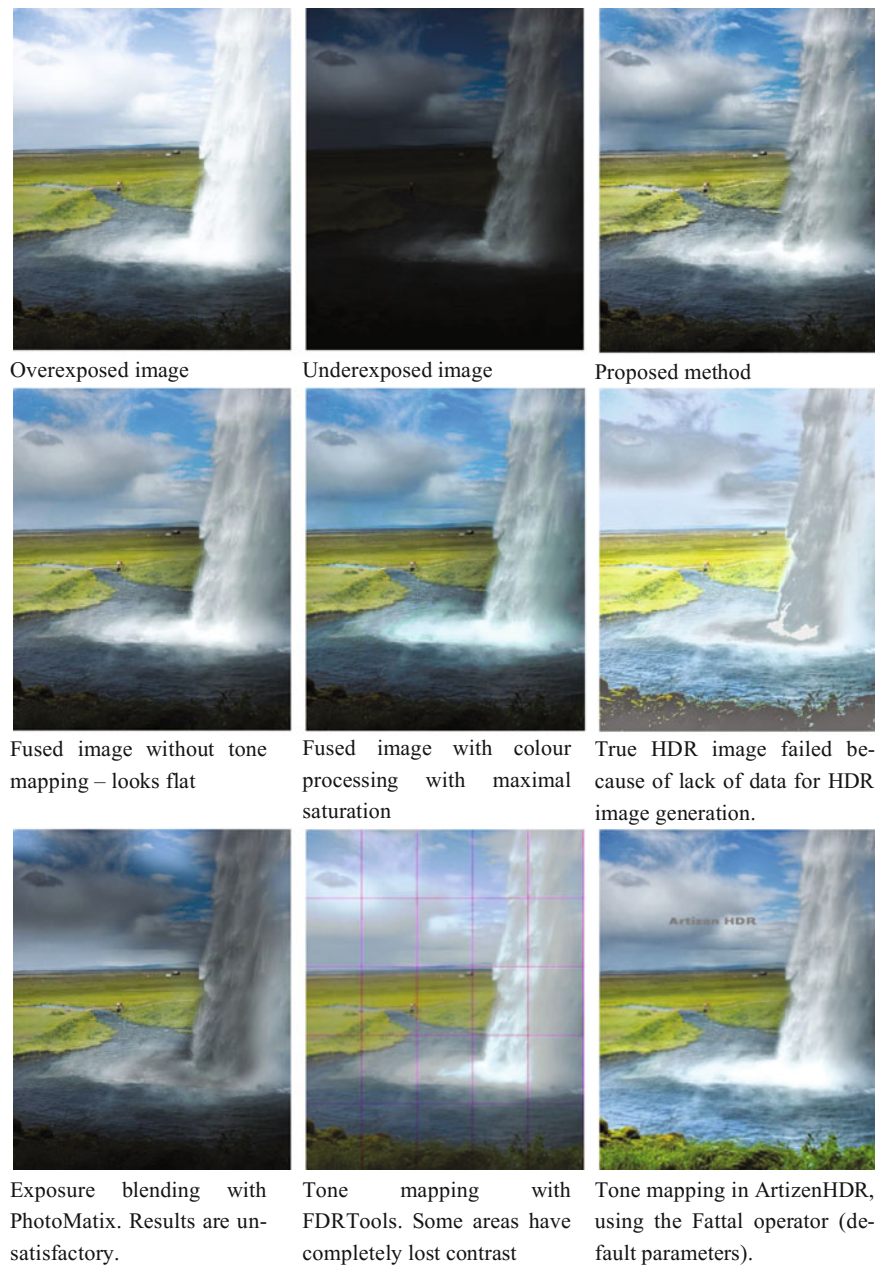


**Fig. 2.10** Results of combining waterfall images



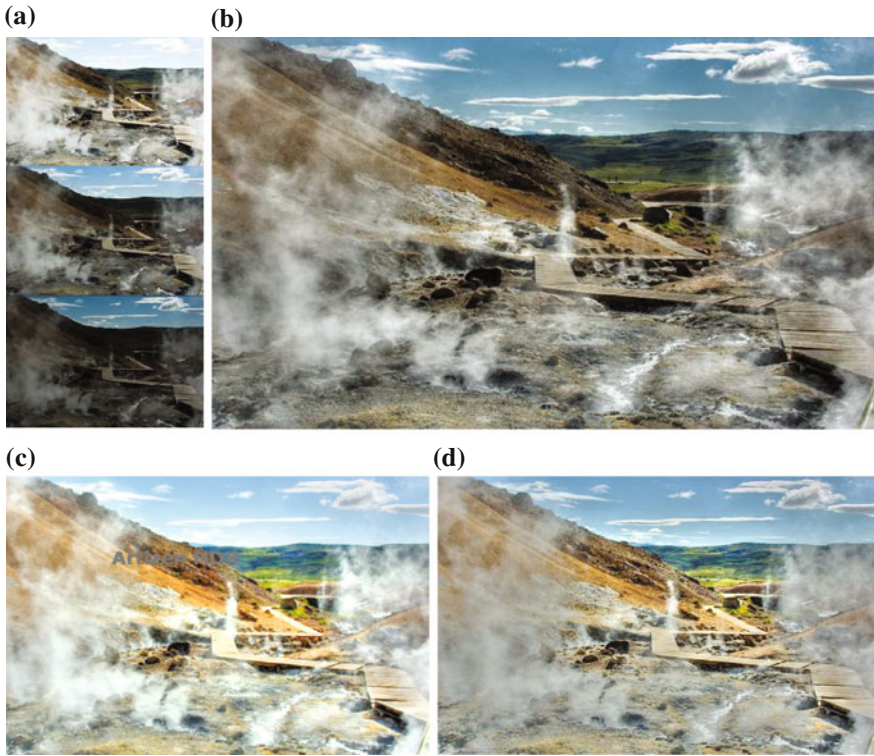


**Fig. 2.11** Results of mapping of a thermal area, including bright vapor trails: **a** input images; **b** resulting fused image; **c** result produced by Artizen HDR (default settings); **d** result produced by Photomatix (default settings)

The developed method has several advantages and disadvantages. The following are among the advantages.

- There is no need for calibration: the number of input images is arbitrary, from 2 to 10 (as opposed to the majority of cited methods).
- An HDR image is not constructed.
- Image interpolation for aligning is performed using image gradients.
- The minimization problem is solved just once.

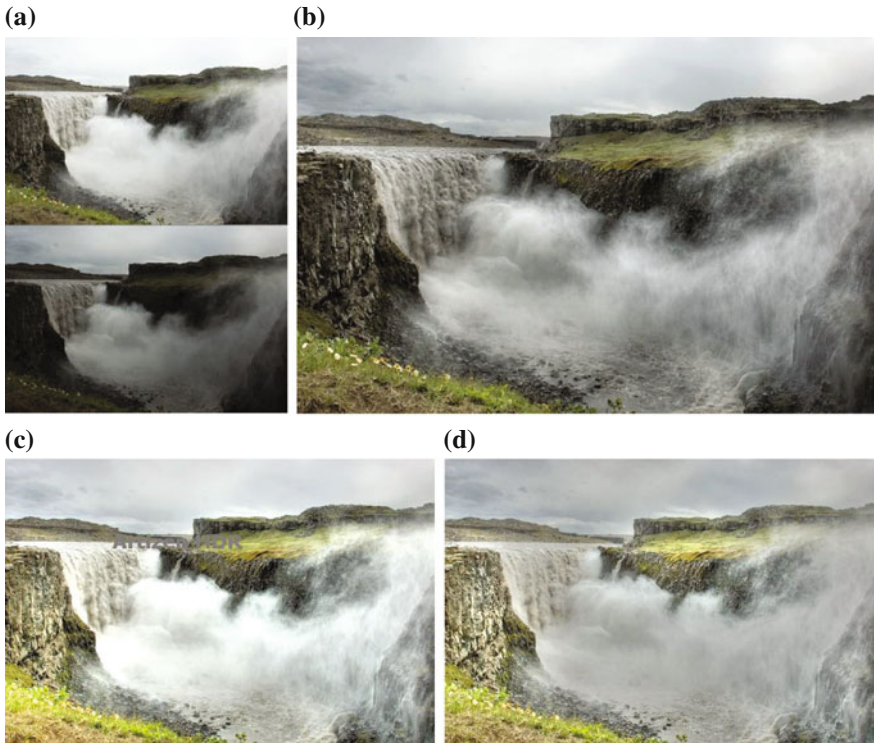


**Fig. 2.12** Results of mapping of waterfall: **a** input images; **b** resulting fused image; **c** result produced by Artizen HDR (default settings); **d** result produced by Photomatix (default settings)

- Processing is performed in YCrCb colour space therefore no extra conversions in case input images are JPEG images.
- New simple scheme of colour mapping.
- Fully automatic.
- The final image is kept as close as possible to the original.



**Fig. 2.13** Example from Photomatix website: **a** input images; **b** results of proposed method; **c** results of Photomatix

The method has the following disadvantages.

- There is a slight halo around strong edges when parameter  $\gamma$  is not set precisely.
- The minimization problem has to be solved.
- An existing halo (for example, around light bulbs) will not be suppressed.



**Fig. 2.14** Example 1 of image processing by proposed method



**Fig. 2.15** Example 2 of image processing by proposed method

Figures 2.14, 2.15, 2.16 and 2.17 present some more results of image fusion.

The quality characteristics of the output image depend, of course, on the number of input images. The greater the quantity of input information, the more details are





Fig. 2.16 Example 3 of image processing by proposed method



Fig. 2.17 Example 4 of image processing by proposed method



Fig. 2.18 Input images



**Fig. 2.19** Left: result with two input images (second and fourth); right: result with five input images (demonstrates significant loss of contrast)



**Fig. 2.20** Input images

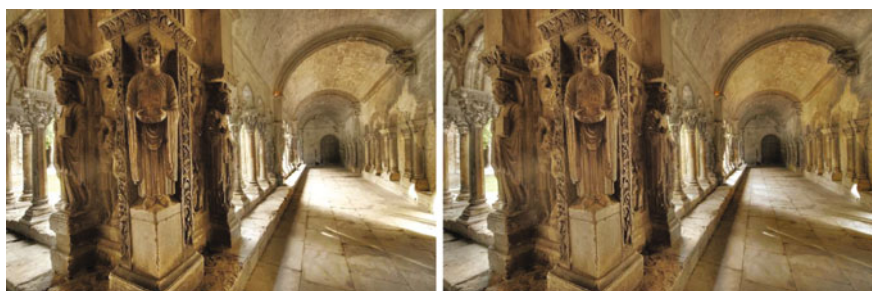


**Fig. 2.21** Left: result with two input images (first and third); right: result with four input images

preserved. However, it results in some loss of contrast. Figures 2.18 and 2.19 demonstrate results with two and five input images. In Figs. 2.20 and 2.21, the difference is not so noticeable.

## References

- Akyuz, A.O., Reinhard, E.: Color appearance in high dynamic range imaging. *SPIE J. Electron. Imaging* **15**(3) (2006)
- Debevec, P., Malik, J.: Recovering high dynamic range radiance maps from photographs. In: *ACM SIGGRAPH 2008 classes*, p. 31. ACM (1998)
- Devlin, K.: A review of tone reproduction techniques. University of Bristol, Tech. Rep. CSTR-02-005 (2002)
- DiCarlo, J., Wandell, B.: Rendering high dynamic range images. In: *Proceedings of the SPIE: Image Sensors*, vol. 3965, pp. 392–401 (2000)
- Durand, F., Dorsey, J.: Fast bilateral filtering for the display of high-dynamic-range images. *ACM Trans Graph (TOG)* **21**(3), 257–266 (2002)
- Fairchild, M.D., Johnson, G.M.: Meet iCAM: an image color appearance model. In: *IS&T/SID 10th Color Imaging Conference* (2002)
- Fairchild, M.D., Johnson, G.M.: Image appearance modelling. In: *Proceedings of IS&T/SPIE Electronic Imaging*, vol. 5007, pp. 149–160 (2003)
- Fattal, R., Lischinski, D., Werman, M.: Gradient domain high dynamic range compression. *ACM Trans. Graph.* **21**(3), 249–256 (2002)
- Ferwerda, J.: Fundamentals of spatial vision. In: *Applications of visual perception in computer graphics, SIGGRAPH'98 Course Notes* (1998)
- Ilie, A., Raskar, R., Yu, J.: Gradient domain context enhancement for fixed cameras. *Int. J. Pattern Recognit. Artif. Intell.* **19**(4), 533–549 (2005)
- Mann, S., Mann, R.: Quantigraphic imaging: estimating the camera response and exposures from differently exposed images. In: *Proceedings of IEEE Conference on Computer Vision and Pattern Recognition*, pp. 842–849 (1998)
- Mann, S., Pickard, R.W.: Being undigital with digital cameras: extending dynamic range by combining differently exposed pictures. In: *Proceedings of IS&T 48th Annual Conference*, pp. 422–428 (1995)
- Pattanaik, S.N., Ferwerda, J.A., Fairchild, M.D., Greenberg, R.W.: A multiscale model of adaptation and spatial vision for realistic image display. In: *ACM SIGGRAPH Computer Graphics Proceedings, Annual Conference Series*, pp. 287–298 (1998)
- Perez, P., Gangnet, M., Blake, A.: Poisson image editing. *ACM Trans. Graph.* **22**(3), 313–318 (2003)
- Raskar, R., Ilie, A., Yu, A.: Image fusion for context enhancement. *NPAR 2004: Third International Symposium on Non Photorealistic Rendering* (2004)
- Reinhard, E., Stark, M., Shirley, P., Ferwerda, J.: Photographic tone reproduction for images. In: *Proceedings of SIGGRAPH 2002, ACM SIGGRAPH*, pp. 267–276 (2002)
- Safonov, I.V., Rychagov, M.N., Kang, K.M., Kim, S.H.: Automatic correction of exposure problems in photo printer. In: *Proceedings of IEEE Tenth International Symposium on Consumer Electronics (ISCE)*, pp. 13–18 (2006)
- Socolinsky, D.: Dynamic range constraints in image fusion and visualization. In: *Proceedings on Signal and Image Processing* (2000)
- Tolstaya, E.V., Rychagov, M.N., Kang, K.M., Kim, S.H.: Fusion of high dynamic range scene photos. In: *Proceedings of IS&T/SPIE Electronic Imaging* (2009)
- Tomasi, C., Manduchi, R.: Bilateral filtering for gray and color images. In: *Proceedings of IEEE Conference on Computer Vision* (1998)
- Vogl, B.: Overview of tone mapping operators and algorithms. <http://dativ.at/logmap/#overview>

Adaptive Image Processing Algorithms for Printing

Safonov, I.V.; Kurilin, I.V.; Rychagov, M.; Tolstaya, E.V.

2018, XVIII, 304 p. 261 illus., 188 illus. in color.,

Hardcover

ISBN: 978-981-10-6930-7